Rapid Communications

Geopotential measurement with a robust, transportable Ca^+ optical clock

Yao Huang,[1,2] Huaqing Zhang,[1,2,3] Baolin Zhang,[1,2,3] Yanmei Hao,[1,2,3] Hua Guan,[1,2,*] Mengyan Zeng,[1,2,3] Qunfeng Chen,[1,2] Yige Lin,[4] Yuzhuo Wang,[4] Shiying Cao,[4] Kun Liang,[4] Fang Fang,[4] Zhanjun Fang,[4] Tianchu Li,[4] and Kelin Gao[1,2,†]

[1]*State Key Laboratory of Magnetic Resonance and Atomic and Molecular Physics, Innovation Academy for Precision Measurement Science and Technology, Chinese Academy of Sciences, Wuhan 430071, China*

[2]*Key Laboratory of Atomic Frequency Standards, Innovation Academy for Precision Measurement Science and Technology, Chinese Academy of Sciences, Wuhan 430071, China*

[3]*University of Chinese Academy of Sciences, Beijing 100049, China*

[4]*National Institute of Metrology, Beijing 100029, China*

(Received 29 June 2020; accepted 20 October 2020; published 18 November 2020)

We present a robust, transportable Ca^+ optical clock, with a systematic uncertainty of 1.3×10^{-17} limited by the black-body radiation (BBR) field evaluation and an uptime rate of >75% over a 20-day period. The clock is then installed in an air-conditioned car trailer, making it more convenient for applications. Referenced to a stationary laboratory clock, geopotential measurements are made with the transportable clock with a total uncertainty of 0.33 m (statistically 0.25 m and systematically 0.22 m) and agree with the spirit level measurement. After being moved >1200 km, the absolute frequency of the Ca^+ optical clock transition is measured as 411 042 129 776 400.41(23) Hz, with a fractional uncertainty of 5.6×10^{-16}, which is about one order of magnitude smaller than our previous measurement. The transportable built can be used for sub-meter-level elevation measurements, comparing intercontinental optical clocks, verifying basic physical theories, etc.

DOI: 10.1103/PhysRevA.102.050802

In the past 20 years, optical clocks have been improved greatly and rapidly in terms of uncertainty and stability, both of which are now more than two orders of magnitude higher than those of the current reference for the definition of the second [1–3]. The uncertainty or stability of the state-of-the-art optical clocks reached the 10^{-18} level or better [4–8]. Optical clocks developed by several different laboratories have been compared with each other through fiber links [9–12], for measuring the frequency ratio of different optical clocks [10,13–18], defining the Standard International (SI) second using optical clocks in the future [19], testing the Lorentz invariance [18,20–24], and searching for the temporal variation of the fundamental physical constants [25–27], etc. Beside application in metrology and verification of basic physical theories, optical clocks can be used in geodesy physics. According to Einstein's theory of general relativity, a clock would run more slowly under a gravitational potential, which is so-called the gravitational red shift; this theoretical prediction has been confirmed by numerous experiments [10,16,28–32]. Therefore, by accurately measuring the frequency difference between two optical clocks at two separate locations, the altitude difference between these two locations can be directly calculated [33]. This, in turn, can greatly help in studying the Earth's shape and mass distributions and precisely determining the global ground elevation network [34]. An accurate global ground elevation network can provide references for gravity prospection; precise coordinates of ground stations for manned space projects, satellites, and missile launches [35]; and key data for defining the second in the future.

For determining the gravity potential, the geometric leveling and the Global Navigation Satellite System (GNSS)/geoid methods are used [34]. When measuring the elevation difference between two locations in two different countries, the reference difference is of the order of meters because the altitude systems of different countries refer to different tidal measurement stations [36]. Therefore, in the measurements between locations that are continental scales away, the geometric leveling method always has relatively low accuracy. By contrast, the GNSS/geoid method requires high-resolution, high-quality gravitational and terrain data. Meanwhile, elevation difference results obtained using the geometric leveling method and the GNSS/geoid method between two locations that are thousands of kilometers apart show decimeter-level differences [35]. Thus, scientists need to use a third method to test the reliability of these results. With the use of optical clocks for elevation measurements, the additive effect of errors caused by the multistep measurements in traditional methods can be avoided; in addition, the measurement accuracy is expected to be further improved by the continuous development and comparison of high-precision optical clocks. However, the above-mentioned high-precision optical clocks can currently be operated only in laboratory environments. To realize practical applications such as for elevation measurement, optical clocks must be made transportable to expand their application scope and eliminate restrictions on their application locations. Therefore, various institutions worldwide are actively developing transportable optical clocks [16,32,37,38]. Grotti *et al.* reported a proof of concept

*guanhua@wipm.ac.cn
†klgao@wipm.ac.cn

 ©2020 American Physical Society

experiment to measure a height difference of ≈1000 m with a transportable Sr optical lattice clock (OLC) [16]. Takamoto *et al.* reported a test of general relativity with a pair of transportable Sr optical lattice clocks [32].

Here we present a transportable Ca^+ optical clock installed in an air-conditioned car trailer, with a systematic uncertainty of 1.3×10^{-17}. Geopotential measurements were made with the transportable clock, both locally with a 100-m-long fiber and remotely over 1200-km distance. Meanwhile, the absolute frequency of the Ca^+ optical clock transition was measured and both locally referenced to a Cs fountain and remotely referenced to SI second through a circular T monthly published by the International Bureau of Weights and Measures (BIPM) [39].

The characteristics of Ca^+ optical clocks differ from those of the OLC described above, and single ions are taken for reference. Therefore, the signal-to-noise ratio is relatively poor and the stability is often one to two orders of magnitude worse than that of the OLC [8,40]. However, a single Ca^+ ion trapped by an electric field under a weak magnetic field is relatively isolated, and therefore there are only negligible systematic shifts for the collisional or Zeeman shift and the total systematic shift is relatively lower, favorable for achieving high precision and reproducibility. The dominating contributor for the systematic shift is the black-body radiation (BBR) effect ($\approx 9 \times 10^{-16}$ at room temperature); however, the uncertainty for the BBR shift can be evaluated to $<1 \times 10^{-16}$ if the BBR field temperature uncertainty can be evaluated to <8 K. The contributors other than the BBR effect only bring in shifts at the 10^{-17} level or even lower [41]. Further, the probability for chemically reaction between Ca^+ and the background gas is very low, and thus the Ca^+ has a long life-time once loaded, enabling continuous work over a long period. All lasers used in Ca^+ optical clocks do not require frequency doubling. Diode lasers delivered by commercial fibers can be used in these clocks: They are inexpensive, their high robustness can improve the operating uptime rate of optical clocks, and their relatively simple structure is conducive for the miniaturization and integration of optical clocks.

Two Ca^+ optical clocks had been built earlier, with uncertainties at the 10^{-17} level [42]. In this study, we remodeled clock 2 to have slightly better accuracy; the laser system and the controlling system were miniaturized and integrated, making the clock transportable. Specific changes can be found in the Supplemental Material [43]. After integrating the transportable optical clock and comparing it to a different optical clock in laboratory environments, the transportable clock was moved to an air-conditioned car trailer for fast and convenient transportation. As shown in Fig. 1, the car trailer has interior dimensions of $4.82 \times 2.3 \times 1.95$ m^3. It has two individual rooms, and the experimental room has a size of $3.05 \times 2.3 \times 1.95$ m^3. The temperatures within the two rooms were independently controlled by air conditioners and temperature detectors, and the peak temperature fluctuations in the experimental room were limited to ±2 K. All components except for the electronics were placed on a 2.4×0.9 m^2 size optical table. During transportation, steel cables were used under the optical table to reduce vibration, and the table was placed under a rigid support after transportation. All equipment used in the optical clock were powered using a vehicle-mounted

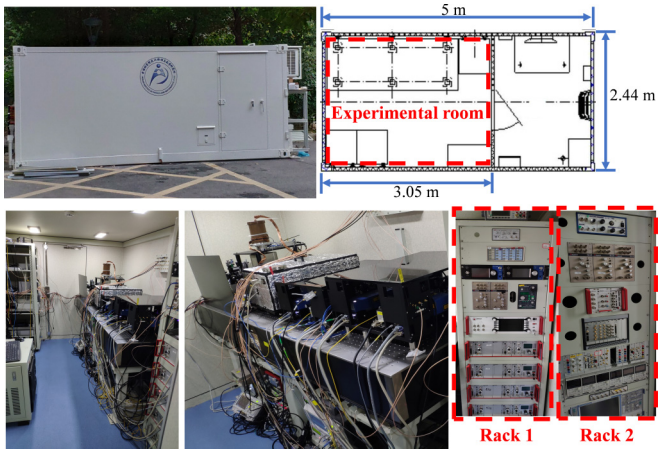

FIG. 1. Transportable Ca^+ optical clock in an air-conditioned car trailer. Top left: outside view of the car trailer. Top right: top view layout of the car trailer. Bottom left: inner view of the car trailer with the transportable clock. Bottom center: physical package and the laser optics (clock laser system not included). Bottom right: electronics.

uninterruptible power supply (UPS) to ensure the continuous operation of the optical clock within half an hour during an unexpected power failure. When the vehicle was running, the UPS was only used to maintain the power supply of the ion pumps and could therefore work continuously for more than 3 days.

Several institutions worldwide have built long-distance fiber comparison systems and performed high-precision frequency comparisons among optical clocks [10,11]; in the above-mentioned studies, detailed systematic uncertainty analyses were conducted for each optical clock. However, because their properties were not examined individually, elevation differences could not be directly calculated from the comparison results of optical clocks; in addition to the gravitational red shift caused by elevation difference, errors or unevaluated systematic uncertainty might also exist. Two optical clocks in two different places must first be moved to the same laboratory for comparison; the elevation difference between these two places can then be calculated from the frequency ratios of the two optical clocks when placed accordingly only after determining the frequency ratio without elevation difference. Therefore, we made a frequency comparison between the transportable clock and the stationary laboratory clock first; the systematic shift evaluations for both clocks was also made. Afterward, the transportable clock was moved to the car trailer, the clock height was made ≈4.3 m higher, and then a frequency comparison between the two clocks and systematic shift evaluations was made once again. After two rounds of clock comparison, the new transportable clock laser was used for a 2-day-long short-term clock run to test the clock stability and reliability. Figure 2 shows the measurement of the frequency difference between the transportable clock and the stationary clock, before and after changing the transportable altitude; the fractional frequency difference change was measured as $4.60(35) \times 10^{-16}$, with statistic uncertainty of 2.7×10^{-17} and systematic uncertainty of 2.3×10^{-17}. Inset shows the Allan deviation of the clock comparisons. According to the general relativity, the

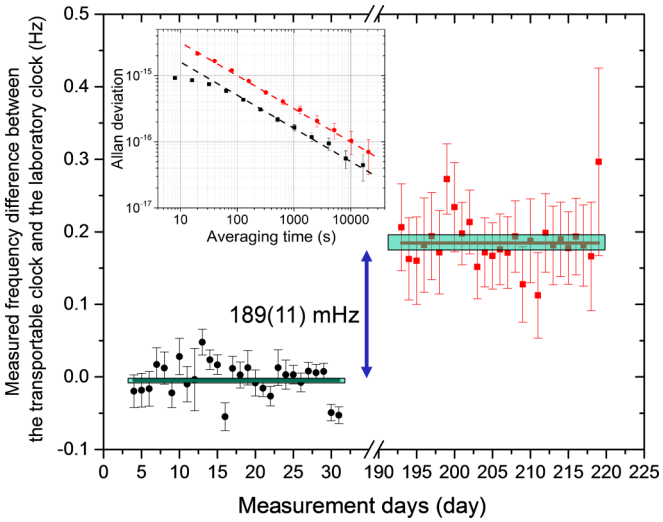

FIG. 2. The measurement of the frequency difference change in Wuhan. The data points shown are systematic shift corrected (gravitational shift excluded); each data point shows the average and the statistical error of the raw data in a day. The black circles on the left represent when the transportable clock was put in the laboratory environment where the two clocks have a height difference of 1 cm, while the red squares on the right represent when the transportable clock was put in the car trailer and the two clocks have a height difference of 4.34(3) m. The black and red horizontal lines and the green-shaded bands shows the weighted mean and the uncertainty of the two data sets, respectively. For the clock comparison at the laboratory environment, a clock laser synchronously probed the two clocks using Ramsey spectroscopy method, with a free evolution time of 40–80 ms [44]. When the transportable clock was moved to the car trailer, Rabi interrogation method was used. For the stationary laboratory clock, probe time was set to 40–80 ms; for the transportable clock, probe time was set as 40 ms. The synchronous probing technique was not used here. Before and after changing the transportable altitude, the frequency difference change was measured as 0.189(11) Hz. Inset: The Allan deviation of the clock comparisons calculated from one day's data. The black points and line represent when both clocks were in the laboratory, whereas red points and line represent when the transportable clock was moved to the car trailer.

altitude change for the transportable clock was calculated as 4.22(33) m, in agreement to the measurement of 4.34(3) m using a spirit level.

The above experiments in Wuhan verified the reproducibility of transportable optical clocks, thereby proving the reliability of the operation of optical clocks after transportation. Afterward, the transportable clock was moved >1200 km from Wuhan to Beijing and settled in the National Institute of Metrology of China (NIM), which maintains a Cs fountain clock NIM5 [45] and a time-keeping clock ensemble regularly reported to International Bureau of Weights and Measures (BIPM). It provides the convenience of simultaneous absolute frequency measurement with direct and indirect comparisons versus SI second. The measurement in Beijing is also a verification for the previous satellite frequency transfer link experiment.

After ≈35 h of moving the trailer, the ion fluoresce signal was detected the next day after arriving in Beijing, and then the systematic shifts were evaluated again. It took <1 month in total before beginning the clock measurements. The total systematic uncertainty was 1.3×10^{-17}, compared to our previous evaluation [41]. For some systematic effects, such as BBR field evaluation, the second-order Doppler shift due to thermal motion, the quadrupole, and the servo, the systematic uncertainties were lower. The temperature of the spectroscopy vacuum chamber was measured as 293.3(1.2) K during the measurement. The temperature variation amplitude was even smaller than in the laboratory environment, where the chamber temperature was measured with an uncertainty of ≈1.5 K [41]. The new FPGA controlling system can rapidly change the laser frequencies and power. During the ion-laser-cooling process, the cooling laser was first far-detuned for a 1-ms-long precooling, and then near-detuned for a 0.7-ms-long more effective Doppler cooling. The thermal motion of the ion was measured to be both weaker and more stable, and thus the second-order Doppler shift and uncertainty due to thermal motion was lower. The clock is referenced to the averaging of multiple selective Zeeman transitions for canceling frequency shifts due to first-order Zeeman, quadrupole, and tensor Stark. However, one cannot simultaneously probe the multiple transitions with only one ion, because when switching between the transitions, the change of the above systematic effects may cause the clock laser to be not perfectly locked to the averaging of the multiple transitions, and thus residual systematic shifts are induced.

In Ref. [41], it took ≈2.3 s of repeating the probing at one transition 15 times, and then the clock laser frequency was changed for probing the next transition. The FPGA controlling system helped to probe each transition only once (takes 70 ms) before switching to the next transition, and the residual systematic shifts were greatly lowered. For servo error, the higher order integrating algorithm was optimized, and both the shift and uncertainty were greatly lowered. The total systematic uncertainty was evaluated as 5.5 mHz, corresponding to a fractional uncertainty of 1.3×10^{-17}, limited by the BBR shift, as shown in Table I.

The vibration environment in the car trailer was one order of magnitude worse than that in the laboratory, and therefore, the transportable clock laser was moved to the laboratory environment and passed through a 100-m-long, phase noise canceled fiber for clock-transition detection. The absolute frequency measurement of the transportable Ca^+ optical clock was then performed both using a frequency link to International Atomic Time (TAI) to provide traceability to the SI second and locally referenced to NIM5 in January 2020. During the 20-day-long measurement, the transportable clock was operated for ≈75% of the period. In the experiment, the laser, whose frequency was stabilized to the ion clock-transition spectrum line, was sent to a comb through a phase noise canceled fiber for frequency measurements. The measurements were made with a homemade Er fiber optical frequency comb.

The SI second traceability link contains five key nodes: the transportable Ca^+ optical clock (OC), a HM as local flywheel oscillator, and real-time realizations of the Coordinated Universal Time UTC(NIM), TAI, and SI second. Four procedures were used to measure the frequency ratios between the consecutive nodes. A femtosecond optical frequency comb system developed by NIM measured the frequency ratio of

TABLE I. Uncertainty budget for the systematic shifts evaluation of the transportable Ca^+ optical clock (OC). Numbers are shown in 10^{-17}.

OC systematic	Shift	Uncertainty
BBR: Temperature	84.2	1.2
BBR coefficient including dynamic correction	0	<0.1
Excess micromotion	0	<0.1
Second-order Doppler, secular motion	−1.5	0.2
ac Stark	0.1	0.1
Residual quadrupole	0	<0.1
Residual first-order Zeeman	0	0.2
Second-order Zeeman	0	<0.1
AOM chirping	0	<0.1
Line pulling	0	<0.1
Collision	0	<0.1
First-order Doppler	0	<0.1
Servo	0	<0.1
OC systematic total	82.8	1.3

the optical and the microwave frequencies from the OC and HM. A dual mixer time difference measurement system was used to perform comparisons between HM and UTC(NIM). In the TAI cooperation, the NIM maintained remote time and frequency comparisons by satellite. The frequency ratio of the UTC(NIM) and TAI are reported monthly in Circular T bulletin by *BIPM*. Similarly, the frequency ratio of TAI and the terrestrial time, a realization of the SI second on the geoid, is also found in the bulletin. The method to evaluate the uncertainties in the TAI link was similar to the work in Refs. [46,47], which can be found in detail in the Supplemental Material [43]. The overall uncertainty of the traceability link was evaluated as 5.0×10^{-16}.

The uncertainty budget for the absolute frequency measurements of the Ca^+ optical clock transition at NIM is shown in Table II. When traced to the NIM5, the absolute frequency of the Ca^+ clock was measured as 411 042 129 776 400.6(5) Hz, limited by the accuracy of the fountain clock. When traced to SI second through the circular T, the measured frequency was 411 042 129 776 400.41(23) Hz (relative uncertainty 5.6×10^{-16}). This measurement has an uncertainty about one order of magnitude smaller than our previous measurement [42]. Without gravitational shift correction, the measurement would be 411 042 129 776 405.35(23) Hz. One of our previous measurements made in Wuhan without gravitational shift correction is 411 042 129 776 403.0(1.1) Hz [42]. The clock frequency difference was then calculated through the above two measurements as 2.35(1.1) Hz. According to general relativity, the altitude difference between the two locations is calculated as 52(25) m, $\approx 1.1\sigma$ different from the GNSS/geoid measurement of 82.3(1.1) m [NIM: 110.3(2) m, Wuhan: 28(1) m].

In conclusion, we present a robust, transportable Ca^+ optical clock with a systematic uncertainty of 1.3×10^{-17} and an uptime rate of >75% over a 20-day-period. The clock was installed in an air-conditioned car trailer, making it more convenient for applications. Referenced to a stationary laboratory clock, geopotential measurements were made with the transportable clock and locally with a 100-m-long fiber; the results agree with the spirit level measurements. These geopotential measurements show our transportable optical clock has an elevation measurement uncertainty of 0.25 m, and it is reliable enough for transportable applications. After it was moved to Beijing, the absolute frequency of the Ca^+ optical clock transition was measured. Thanks to the high uptime rate, the uncertainty was about one order of magnitude smaller than our previous measurement, and comparable to the best previously reported measurements. Plans for the measurement of the height difference between Wuhan and NIM have been made: With the fiber or satellite links, the uncertainty is expected to be less than the meter level. The transportable optical clock also can be used for comparing intercontinental optical clocks, verifying basic physical theories, etc. Owing to the limited stability of the transportable clock laser, the stability of the transportable optical clock still needs improvement to be comparable with laboratory optical clocks. In the future,

TABLE II. Uncertainty budget for the absolute frequency measurements of the Ca^+ optical clock transition in NIM. Numbers are shown in 10^{-17}.

Traced to SI second	Unc.	Traced to NIM5	Unc.
Statistical	25		25
OC Systematic	1.3		1.3
Traceability link	50	NIM5 accuracy	107
Gravitational	2		2
Total	56		110

if comparing the transportable optical clock to optical clocks, e.g., comparison with the Sr optical lattice clock of NIM [48], it needs higher stability requirements that, in turn, can provide more precise elevation measurement results in the same amount of time. Improvement of the transportable clock laser need to be made in our next development step, with stability close to the 10^{-16} level at an averaging time of $\approx$10 s, after subtraction of linear drift. We aim to operate the entire optical clock, including the clock laser, in the car trailer to reduce the recovery time after moving the optical clock, as every measurement location does not have an appropriate laboratory environment for placing the transportable clock laser. Because the vibration environment is worse in the car trailer than in the laboratory, methods to reduce the vibration sensitivity of the cavity need to be developed. We also plan to put the ion trap vacuum chamber into an aluminium box and temperature stabilize the box with a chilled water pump. This would reduce the BBR shift uncertainty to the low 10^{-18} level. In addition, the robustness and ease of use of the optical clock need to be further improved by optimizing the automated optical clock locking software.

We thank Chaohui Ye, Jun Luo, Longsheng Ma, Yanyi Jiang, Huanyao Sun, Aimin Zhang, and Yuan Gao for help and fruitful discussion. This work is supported by the National Key R&D Program of China (Grants No. 2017YFA0304404, No. 2017YFA0304401, No. 2018YFA0307500, and No. 2017YFF0212003), the Natural Science Foundation of China (Grants No. 91736310, No. 61905231, No. 11774388, and No. 11634013), the Strategic Priority Research Program of the Chinese Academy of Sciences (Grant No. XDB21030100), CAS Youth Innovation Promotion Association (Grants No. 2018364 and No. Y201963), Hubei Province Science Fund for Distinguished Young Scholars (Grant No. 2017CFA040), and the K. C. Wong Education Foundation.

Y.H. and H.Z. contributed equally to this work.

[1] T. P. Heavner, E. A. Donley, F. Levi, G. Costanzo, T. E. Parker, J. H. Shirley, N. Ashby, S. Barlow, and S. R. Jefferts, Metrologia **51**, 174 (2014).

[2] R. Li, K. Gibble, and K. Szymaniec, Metrologia **48**, 283 (2011).

[3] S. Weyers, V. Gerginov, N. Nemitz, R. Li, and K. Gibble, Metrologia **49**, 82 (2012).

[4] S. M. Brewer, J. S. Chen, A. M. Hankin, E. R. Clements, C. W. Chou, D. J. Wineland, D. B. Hume, and D. R. Leibrandt, Phys. Rev. Lett. **123**, 033201 (2019).

[5] T. Nicholson, S. L. Campbell, R. B. Hutson, G. E. Marti, B. J. Bloom, R. L. McNally, W. Zhang, M. D. Barrett, M. S. Safronova, G. F. Strouse *et al.*, Nat. Commun. **6**, 6869 (2015).

[6] I. Ushijima, M. Takamoto, M. Das, T. Ohkubo, and H. Katori, Nat. Photon. **9**, 185 (2015).

[7] N. Huntemann, C. Sanner, B. Lipphardt, C. Tamm, and E. Peik, Phys. Rev. Lett. **116**, 063001 (2016).

[8] W. F. McGrew, X. Zhang, R. J. Fasano, S. A. Schäffer, K. Beloy, D. Nicolodi, R. C. Brown, N. Hinkley, G. Milani, M. Schioppo *et al.*, Nature (London) **564**, 87 (2018).

[9] D. Calonico, E. K. Bertacco, C. E. Calosso, C. Clivati, G. A. Costanzo, M. Frittelli, A. Godone, A. Mura, N. Poli, D. V. Sutyrin *et al.*, Appl. Phys. B **117**, 979 (2014).

[10] T. Takano, M. Takamoto, I. Ushijima, N. Ohmae, T. Akatsuka, A. Yamaguchi, Y. Kuroishi, H. Munekane, B. Miyahara, and H. Katori, Nat. Photon. **10**, 662 (2016).

[11] C. Lisdat, G. Grosche, N. Quintin, C. Shi, S. M. F. Raupach, C. Grebing, D. Nicolodi, F. Stefani, A. Al-Masoudi, S. Dörscher *et al.*, Nat. Commun. **7**, 12443 (2016).

[12] K. Predehl, G. Grosche, S. M. F. Raupach, S. Droste1, O. Terra, J. Alnis1, Th. Legero, T. W. Hänsch, Th. Udem, R. Holzwart *et al.*, Science **336**, 441 (2012).

[13] F.-L. Hong, M. Musha, M. Takamoto, H. Inaba, S. Yanagimachi, A. Takamizawa, K. Watabe, T. Ikegami, M. Imae, Y. Fujii *et al.*, Opt. Lett. **34**, 692 (2009).

[14] A. Yamaguchi, M. Fujieda, M. Kumagai, H. Hachisu, S. Nagano, Y. Li, T. Ido, T. Takano, M. Takamoto, and H. Katori, Appl. Phys. Expr. **4**, 082203 (2011).

[15] H. Hachisu, M. Fujieda, S. Nagano, T. Gotoh, A. Nogami, T. Ido, St. Falke, N. Huntemann, C. Grebing, B. Lipphardt *et al.*, Opt. Lett. **39**, 4072 (2014).

[16] J. Grotti, S. Koller, S. Vogt, S. Häfner, U. Sterr, C. Lisdat, H. Denker, C. Voigt, L. Timmen, A. Rolland *et al.*, Nat. Phys. **14**, 437 (2018).

[17] K. Matsubara, H. Hachisu, Y. Li, S. Nagano, C. Locke, A. Nogami, M. Kajita, K. Hayasaka, T. Ido, and M. Hosokawa, Opt. Express **20**, 22034 (2012).

[18] K. Beloy, M. I. Bodine, T. Bothwell, S. M. Brewer, S. L. Bromley, J.-S. Chen, J.-D. Deschênes, S. A. Diddams, R. J. Fasano, T. M. Fortier *et al.*, arXiv:2005.14694.

[19] F. Riehle, P. Gill, F. Arias, and L. Robertsson, Metrologia **55**, 188 (2018).

[20] S. Blatt, A. D. Ludlow, G. K. Campbell, J. W. Thomsen, T. Zelevinsky, M. M. Boyd, J. Ye, X. Baillard, M. Fouché, R. Le Targat *et al.*, Phys. Rev. Lett. **100**, 140801 (2008).

[21] R. Le Targat, L. Lorini, Y. Le Coq, M. Zawada, J. Guéna, M. Abgrall, M. Gurov, P. Rosenbusch, D. G. Rovera, B. Nagórny *et al.*, Nat. Commun. **4**, 2109 (2013).

[22] R. Schwarz, S. Dörscher, A. Al-Masoudi, E. Benkler, T. Legero, U. Sterr, S. Weyers, J. Rahm, B. Lipphardt, and C. Lisdat, Phys. Rev. Res. **2**, 033242 (2020).

[23] C. Sanner, N. Huntemann, R. Lange, C. Tamm, E. Peik, M. S. Safronova, and S. G. Porsev, Nature (London) **567**, 204 (2019).

[24] P. Delva, J. Lodewyck, S. Bilicki, E. Bookjans, G. Vallet, R. LeTargat, P. E. Pottie, C. Guerlin, F. Meynadier, C. LePoncin-Lafitte *et al.*, Phys. Rev. Lett. **118**, 221102 (2017).

[25] T. Rosenband, D. B. Hume, P. O. Schmidt, C. W. Chou, A. Brusch, L. Lorini, W. H. Oskay, R. E. Drullinger, T. M. Fortier, J. E. Stalnaker *et al.*, Science **319**, 1808 (2008).

[26] R. M. Godun, P.?B.?R. Nisbet-Jones, J.?M. Jones, S.?A. King, L.?A.?M. Johnson, H.?S. Margolis, K. Szymaniec, S.?N. Lea, K. Bongs, and P. Gill, Phys. Rev. Lett. **113**, 210801 (2014).

[27] N. Huntemann, B. Lipphardt, C. Tamm, V. Gerginov, S. Weyers, and E. Peik, Phys. Rev. Lett. **113**, 210802 (2014).

[28] R. V. Pound and J. L. Snider, Phys. Rev. **140**, B788 (1965).
[29] P. Delva, N. Puchades, E. Schönemann, F. Dilssner, C. Courde, S. Bertone, F. Gonzalez, A. Hees, Ch. Le Poncin-Lafitte, F. Meynadier *et al.*, Phys. Rev. Lett. **121**, 231101 (2018).
[30] S. Herrmann, F. Finke, M. Lulf, O. Kichakova, D. Puetzfeld, D. Knickmann, M. List, B. Rievers, G. Giorgi, C. Günther *et al.*, Phys. Rev. Lett. **121**, 231102 (2018).
[31] C. W. Chou, D. B. Hume, T. Rosenband, and D. J. Wineland, Science **329**, 1630 (2010).
[32] M. Takamoto, I. Ushijima, N. Ohmae, T. Yahagi, K. Kokado, H. Shinkai, and H. Katori, Nat. Photon. **10**, 1038 (2020).
[33] A. Bjerhammar, Tellus **27**, 97 (1975).
[34] T. Mehlstäubler, G Grosche, C. Lisdat, P. O. Schmidt, and H. Denke, Rep. Prog. Phys. **81**, 064401 (2018).
[35] H. Denker, L. Timmen, C. Voigt, S. Weyers, E. Peik, H. S. Margolis, P. Delva, P. Wolf, and G. Petit, J. Geod. **92**, 487 (2017).
[36] D. A. Smith, S. A. Holmes, X. Li, Sébastien Guillaume, Y. M. Wang, B. Bürki, D. R. Roman, and T. M. Damiani, J. Geod. **87**, 885 (2013).
[37] J. Cao, P. Zhang, J. Shang, K. Cui, J. Yuan, S. Chao, S. Wang, H. Shu, and X. Huang, Appl. Phys. B **123**, 112 (2017).
[38] S. Origlia, M. S. Pramod, S. Schiller, Y. Singh, K. Bongs, R. Schwarz, A. Al-Masoudi, S. Dörscher, S. Herbers, and S. Häfner, Phys. Rev. A **98**, 053443 (2018).
[39] https://www.bipm.org/en/bipm-services/timescales/time-ftp/Circular-T.html.
[40] E. Oelker, R. B. Hutson, C. J. Kennedy, L. Sonderhouse, T. Bothwell, A. Goban, D. Kedar, C. Sanner, J. M. Robinson, G. E. Marti *et al.*, Nat. Photon. **13** 714 (2019).
[41] Y. Huang, H. Guan, M. Zeng, L. Tang, and K. Gao, Phys. Rev. A **99**, 011401(R) (2019).
[42] Y. Huang, H. Guan, P. Liu, W. Bian, L. Ma, K. Liang, T. Li, and K. Gao, Phys. Rev. Lett. **116**, 013001 (2016).
[43] See Supplemental Material at http://link.aps.org/supplemental/10.1103/PhysRevA.102.050802 for details about the efforts to make the laboratory optical clock transportable, the comparison of two Ca^+ optical clocks in Wuhan, and the SI second traceability link in NIM, Beijing.
[44] B. Zhang, Y. Huang, Y. Hao, H. Zhang, M. Zeng, H. Guan, and K. Gao, J. Appl. Phys. **128**, 143105 (2020).
[45] F. Fang, M.Li, P.Lin, W.Chen, N.Liu, Y.Lin, P.Wang, K.Liu, R.Suo, and T.Li, Metrologia **52**, 454 (2015).
[46] H. Hachisu, G. Petit, F. Nakagawa, Y. Hanado, and T. Ido, Opt. Expr. **25**, 8511 (2017).
[47] C. F. A. Baynham, R. M. Godun, J. M. Jones, S. A. King, P. B. R. Nisbet-Jones, F. Baynes, A. Rolland, P. E. G. Baird, K. Bongs, P. Gill *et al.*, J. Mod. Opt. **65**, 585 (2017).
[48] Y.-G. Lin, Q. Wang, Y. Li, F. Meng, B.-K. Lin, E.-J. Zang, Z. Sun, F. Fang, T.-C. Li, and Z.-J. Fang, Chin. Phys. Lett. **32**, 090601 (2015).